

LABORATORY STUDY



Disulfiram ameliorates ischemia/reperfusion-induced acute kidney injury by suppressing the caspase-11-GSDMD pathway

Qiaoting Cai^{a,b,c}, Zhaoxing Sun^{a,b,c}, Sujuan Xu^{a,b,c}, Xiaoyan Jiao^{a,b,c,d}, Shulan Guo^{a,b,c},
Yingxiang Li^{a,b,c}, Huan Wu^{a,b,c} and Xiaofang Yu^{a,b,c,d}

^aDepartment of Nephrology, Zhongshan Hospital, Fudan University, Shanghai, China; ^bShanghai Medical Center for Kidney, Shanghai, China; ^cShanghai Key Laboratory of Kidney and Blood Purification, Shanghai, China; ^dShanghai Institute of Kidney and Dialysis, Shanghai, China

ABSTRACT

Acute kidney injury (AKI) is a serious condition with high mortality. The most common cause is kidney ischemia/reperfusion (IR) injury, which is thought to be closely related to pyroptosis. Disulfiram is a well-known alcohol abuse drug, and recent studies have shown its ability to mitigate pyroptosis in mouse macrophages. This study investigated whether disulfiram could improve IR-induced AKI and elucidated the possible molecular mechanism. We generated an IR model in mouse kidneys and a hypoxia/reoxygenation (HR) injury model with murine tubular epithelial cells (MTECs). The results showed that IR caused renal dysfunction in mice and triggered pyroptosis in renal tubular epithelial cells, and disulfiram improved renal impairment after IR. The expression of proteins associated with the classical pyroptosis pathway (Nucleotide-binding oligomeric domain (NOD)-like receptor protein 3 (NLRP3), apoptosis-related specific protein (ASC), caspase-1, N-GSDMD) and nonclassical pyroptosis pathway (caspase-11, N-GSDMD) were upregulated after IR. Disulfiram blocked the upregulation of nonclassical but not all classical pyroptosis pathway proteins (NLRP3 and ASC), suggesting that disulfiram might reduce pyroptosis by inhibiting the caspase-11-GSDMD pathway. *In vitro*, HR increased intracellular ROS levels, the positive rate of PI staining and LDH levels in MTECs, all of which were reversed by disulfiram pretreatment. Furthermore, we performed a computer simulation of the TIR domain of TLR4 using homology modeling and identified a small molecular binding energy between disulfiram and the TIR domain. We concluded that disulfiram might inhibit pyroptosis by antagonizing TLR4 and inhibiting the caspase-11-GSDMD pathway.

Abbreviations: AKI: acute kidney injury; ANOVA: analysis of variance; ASC: apoptosis-related specific protein; BCA: bicinchoninic acid; BUN: blood urea nitrogen; CCK8: cell counting kit 8; DAMPs: damage-related molecular patterns; DCFH-DA: dichlorodihydrofluorescein diacetate; ECL: enhanced chemiluminescence; GSDMD: gasdermin D; HE: hematoxylin-eosin; HR: hypoxia/reoxygenation; IF: immunofluorescence; IL-10: interleukin-10; IL-18: interleukin-18; IL-1 β : interleukin-1 β ; IL-4: interleukin-4; IR: ischemia/reperfusion; LDH: lactate dehydrogenase; LPS: lipopolysaccharide; MTECs: murine tubular epithelial cells; NLRP3: nucleotide-binding oligomeric domain (NOD)-like receptor protein 3; PAMPs: pathogen-associated molecular patterns; PAS: periodic acid-Schiff; RIPA: radio immunoprecipitation assay; ROS: reactive oxygen species; Scr: serum creatinine; SEM: standard error of mean; TIR: toll and interleukin-1 receptor-like; TLR4: toll-like receptor 4

ARTICLE HISTORY

Received 20 December 2021
Revised 16 June 2022
Accepted 29 June 2022

KEYWORDS

Kidney IR injury; pyroptosis; disulfiram; caspase-11; GSDMD



Introduction

Acute kidney injury (AKI) is recognized as a critical complication in 10–15% of hospitalized patients [1], resulting in high mortality of up to 23.9% [2]. Despite current progress in understanding AKI pathophysiology, effective strategies and drug therapies for AKI are still not available.

Kidney ischemia/reperfusion (IR) injury is the primary cause of AKI and may result from a variety of

conditions, such as sepsis, thromboembolic events, circulatory shock and bypass surgery. A reduction in the glomerular filtration rate occurs during IR injury, which eventually leads to kidney function decline and is independently associated with an increased risk of death [3].

It has been previously reported that apoptosis and necrosis are the major pathological processes associated with kidney IR injury. However, the inhibition of

CONTACT Xiaofang Yu  yu.xiaofang@zs-hospital.sh.cn  Department of Nephrology, Zhongshan Hospital, Shanghai Medical College, Fudan University, NO 180 Fenglin Road, 200032, Shanghai, China

© 2022 The Author(s). Published by Informa UK Limited, trading as Taylor & Francis Group.

This is an Open Access article distributed under the terms of the Creative Commons Attribution-NonCommercial License (<http://creativecommons.org/licenses/by-nc/4.0/>), which permits unrestricted non-commercial use, distribution, and reproduction in any medium, provided the original work is properly cited.

apoptosis and necrosis alone did not completely prevent IR-induced AKI [4]. Recent studies have demonstrated that pyroptosis is involved in the development of kidney IR injury and that suppressing pyroptosis could protect the kidney against IR injury [5,6]. Gasdermin D (GSDMD) is a key effector protein in pyroptosis. The N-terminus of GSDMD is produced by active caspase-1 or caspase-11, which forms cytomembrane pores that cause cell death and the release of the mature forms of IL-1 β and IL-18 [7,8].

Disulfiram has been widely used as a second-line alcohol-abuse treatment for 65 years [9]. As a model for drug repurposing, disulfiram has also been shown to be an anticancer drug that sensitizes cancer cells that are resistant to cisplatin [10]. More recently, disulfiram was shown to inhibit pyroptosis by blocking GSDMD pore formation in immortalized murine bone marrow-derived macrophages [11]. However, it is not clear whether disulfiram could attenuate the damage induced by kidney IR injury or the potential mechanism.

In this study, we investigated the effect of disulfiram on kidney IR injury and illuminated the underlying molecular mechanisms. Our results showed that disulfiram could regulate pyroptosis *via* the caspase-11-GSDMD axis in the kidney to play a protective role against kidney IR injury.

Methods

Animals and AKI models

Male C57BL/6 mice (8–10 weeks old, 20–25 g) were purchased from Shanghai Jihui Laboratory Animal Care Co., Ltd. (Shanghai, China). The mice were housed in a temperature- and humidity-controlled environment with a 12:12-h light/dark cycle (light on at 07:00 a.m.) and were given free access to food and water at the Animal Center of Fudan University. The animals were randomized into three groups: sham group ($n=6$), IR group ($n=6$), and IR + DSF group ($n=6$). Kidney IR injury was induced by bilateral kidney pedicle clamping for 30 min, followed by reperfusion for 24 h. Finally, the mice were sacrificed, and the kidney tissues were carefully collected for subsequent experiments. The sham group underwent all surgical procedures except vascular occlusion. The IR + DSF group received an intraperitoneal injection of disulfiram (50 mg/kg) for 3 consecutive days prior to surgery. The sham group and IR group were intraperitoneally injected with the same volume of the solvent corn oil. The animal study was reviewed and approved by the Animal Ethics Committee of Zhongshan Hospital, Fudan University.

Cell culture and treatment

Mouse tubular epithelial cells (MTECs) were cultured in DMEM High Glucose media (Gibco, USA) supplemented with 10% FBS (Gibco, USA) in 5% CO₂ and 95% air at 37 °C. To induce the hypoxia/reoxygenation (HR) model, cells in the HR group were cultured in a hypoxic incubator with 1% O₂, 94% N₂ and 5% CO₂ for 24 h. After hypoxia, the cells were transferred to a normoxic incubator for 2 h. Cells in the HR + DSF group were pretreated with disulfiram (0.5 μ M) for 2 h before hypoxia treatment.

Serum creatinine analysis

Blood samples were left to stand for 2 h at room temperature and then centrifuged for 10 min at 3,000 rpm to harvest serum. Serum samples were stored at –20 °C until analysis. Serum creatinine (Scr) and blood urea nitrogen (BUN) levels were measured by the QuantiChrom™ Creatinine Assay Kit and QuantiChrom™ Urea Assay Kit (BioAssay Systems, USA) with a microplate reader in the Nephropathy Laboratory of Fudan University Zhongshan Hospital.

Histological examination

Kidney sections were embedded in paraffin, sectioned, and then stained with hematoxylin-eosin (HE) and periodic acid-Schiff (PAS). Bright field images of kidney tissues were acquired using a Leica microscope with 10 \times and 40 \times objectives.

Western blotting

Mouse kidney tissue or MTECs were lysed in RIPA buffer with PMSF and phosphatase inhibitors (RIPA:PMSF:phosphatase inhibitors = 100:1:1). The protein concentrations were determined using a BCA Protein Assay Kit (Beyotime, China). The protein samples were then transferred to PVDF membranes (Millipore, Sigma). The following primary antibodies were used: Gasdermin D (Abcam, UK), caspase-1 (Abcam, UK), caspase-11 (Abcam, UK), IL-1 β (CST, USA), IL-18 (Proteintech, USA), TLR4 (Proteintech, USA), NLRP3 (Abcam, UK), ASC (Abcam, UK), and β -actin (GeneTex, USA). Anti-mouse or anti-rabbit secondary antibodies (Jackson ImmunoResearch, USA) were used to bind the primary antibodies at room temperature for 1 h. Signals were developed with ECL Western blot detection reagents (Thermo Fisher Scientific, USA). Finally, quantification was performed using ImageJ

v1.8.0 software (National Institutes of Health, Bethesda, MD, USA).

Real-time quantitative PCR

Total RNA was harvested by TRIzol reagent (Sigma, USA). Reverse transcription was performed using PrimeScript RT Master Mix (Takara, Japan). Quantitative real-time PCR was performed with TB Green® Premix Ex Taq™ II (Takara, Japan) on a 7500 PCR instrument (Thermo Fisher Scientific, USA). The primers used were as follows:

Gene	Primers
β-Actin	Forward: CATTGCTGACAGGATGCAGAAGG Reverse: TGCTGGAAGGTGGACAGTGAGG
IL-1β	Forward: TGGACCTTCCAGGATGAGGACA Reverse: GTTCATCTCGGAGCCTTGTAGTG
IL-18	Forward: GACAGCCTGTGTTTCGAGGATATG Reverse: TGTCTTACAGGAGAGGGTAGAC
IL-4	Forward: ATCATCGGCATTTTGAACGAGGTC Reverse: ACCTTGGGAAGCCCTACAGACGA
IL-10	Forward: CGGGAAGACAATAACTGCACCC Reverse: CGGTTAGCAGTATGTTGCCAGC

Immunofluorescence (IF) analysis

IF analysis was performed on paraffin-embedded sections. Sections were deparaffinized in xylene before being heated in citrate-EDTA antigen retrieval solution (Beyotime, China) for antigen retrieval and blocked with 1% BSA. The primary antibodies used for IF analysis were caspase-11 (Santa Cruz, USA) and GSDMD (Abcam, UK). Primary antibodies were incubated at 4 °C overnight. After being washed, the sections were incubated with Alexa Fluor 488 dye-labeled anti-rabbit IgG or Alexa Fluor 594 dye-labeled anti-mouse IgG (Beyotime, China). Finally, the sections were sealed with Antifade Mounting Medium with DAPI (Beyotime, China). Images were visualized using a confocal microscope (Olympus, Japan).

Transmission electron microscopy

The samples were fixed in 2.5% glutaraldehyde in PBS buffer (Servicebio, China). The proximal convoluted tubule section was cut into cubes ($\leq 1 \text{ mm}^3$) before being sent to Servicebio (Wuhan, China) for ultrastructural analysis.

Cell proliferation assay

A Cell Counting Kit 8 (CCK8) (Dojindo, Japan) was used to analyze cell viability. A total of 100 μl of the MTEC

suspension ($5 \times 10^5/\text{mL}$) was inoculated in a 96-well plate. Cells were cultured in the incubator for an appropriate time after the indicated steps, and then 10 μl of CCK8 solution was added to each well 30 min prior to testing. After incubation, the absorbance at 450 nm was determined using a microplate reader.

ROS determination

Intracellular ROS were measured by a ROS assay kit (Beyotime, China). Cells were labeled with 10 μM DCFH-DA for 20 min before being analyzed. Then, the plates were washed three times with serum-free media to remove excess DCFH-DA. After trypsin digestion, the cells were collected. Flow cytometry was used to measure intracellular ROS with excitation at 488 nm and emission at 525 nm.

LDH release

Six-well plates were centrifuged at $400 \times g$ for 5 min to collect the cell culture supernatant. The LDH release percent in the supernatant was determined using an LDH Cytotoxicity Assay Kit (Beyotime, China).

Molecular docking analysis

Molecular docking calculations were conducted with the Yinfo Cloud Computing Platform (<https://cloud.yinfotek.com/>). The 3D structure of disulfiram was constructed with energy minimization in the MMFF94 force field. The TIR domain sequence of the mouse TLR4 protein was obtained from the UniProt KB database, and then the crystal structure of the TIR domain was obtained by homology modeling on the SWISS-MODEL website (<https://swissmodel.expasy.org>). The crystal ligand was used to define the binding pocket. The DOCK 6.9 [12,13] program was used to execute semiflexible docking, and output poses were evaluated by the Grid scoring function.

Statistical analyses

GraphPad Prism software version 8.0 was used for all statistical analyses. All results are expressed as the means \pm SEM. The data were analyzed by analysis of variance (ANOVA) and Bonferroni's posttest comparisons. *P* values < 0.05 were considered statistically significant.

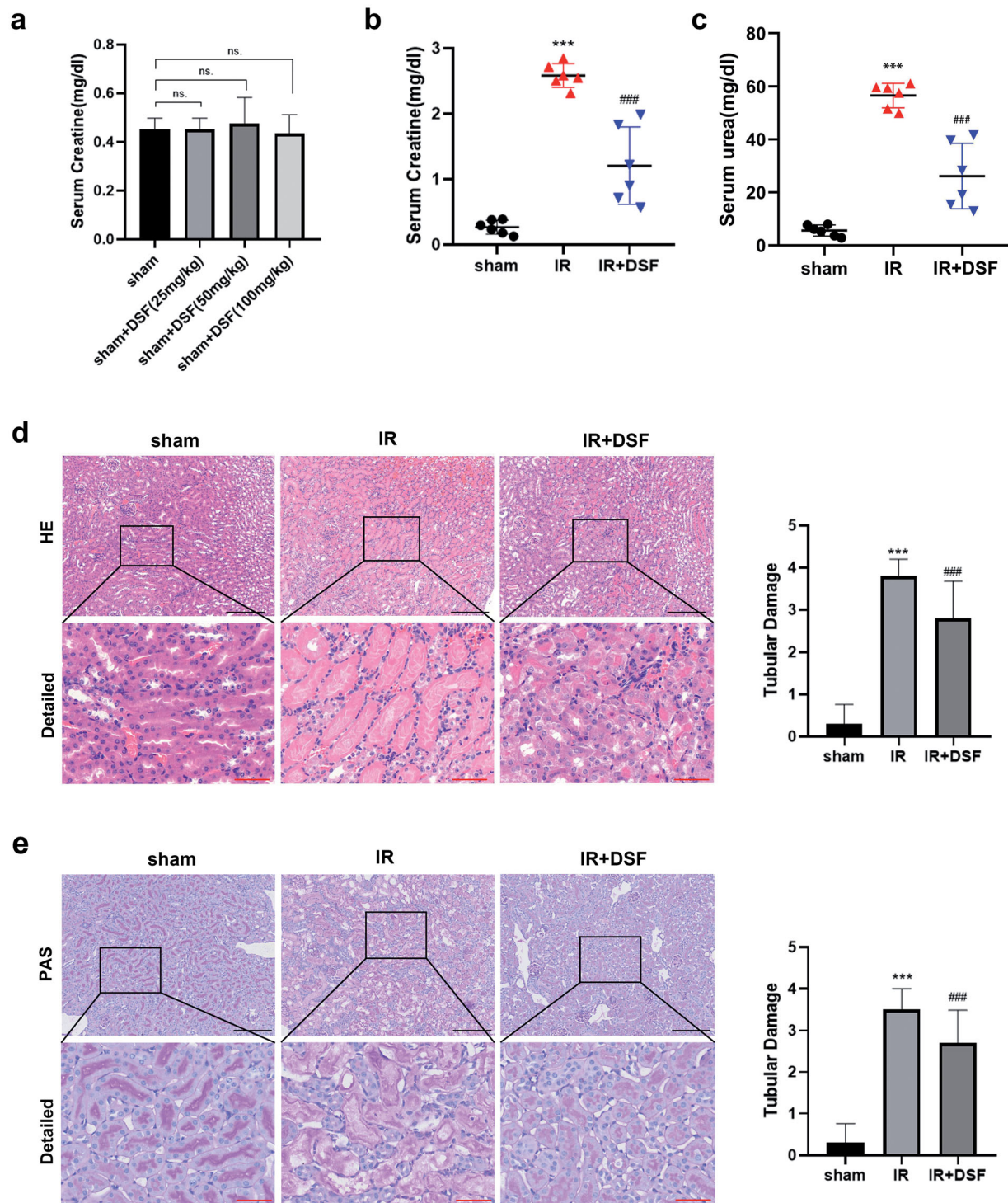


Figure 1. Disulfiram attenuated renal dysfunction and pathological injury in IR-induced AKI. (a, b, c) Serum creatinine (Scr) and blood urea nitrogen (BUN) levels were measured in each group. Each bar represents the mean \pm SEM of the independent experiments. (d) Representative HE staining of renal tubular epithelial cells. A microscope with 10 \times and 40 \times objectives was used to capture the images. Scale bar: black 200 μ m, red 50 μ m. (e) Representative PAS staining of renal tubular epithelial cells. A microscope with 10 \times and 40 \times objectives was used to capture the images. Scale bar: black 200 μ m, red 50 μ m. $n = 6$ per group. *** $P < 0.001$ vs. sham; ### $P < 0.001$ vs. IR. ns, no significance.

Results

Effects of disulfiram on renal function and structural changes after IR injury in vivo

To exclude the effect of disulfiram itself on mice, we established the sham + DSF group in the preliminary experiment, and then we measured the creatinine levels of the sham group and sham + DSF group (including 25 mg/kg DSF, 50 mg/kg DSF and 100 mg/kg DSF). The results showed that there was no significant difference in creatinine levels between the sham group and sham + DSF group, indicating that disulfiram did not damage the renal function of mice (Figure 1a).

After establishing kidney IR injury in mice, we measured the serum levels of Scr and BUN. The IR group showed higher serum Scr and BUN levels than the sham group, and pretreatment with disulfiram decreased the levels of Scr and BUN in contrast to those in the IR group (Figures 1b and c). According to the HE and PAS staining results, the kidneys in the IR group exhibited widespread degenerative changes in tubular epithelial cells, such as tubular dilation, brush border loss and protein cast formation. In contrast to those in the IR group, fewer pathological changes were noted in tubular epithelial cells in the IR + DSF group (Figures 1d and f). Thus, disulfiram pretreatment could attenuate IR-induced renal dysfunction and tubular structure failure.

Disulfiram attenuated proximal tubular cell pyroptosis following IR injury

During ischemic progression, pyroptosis plays a vital role in IR-induced AKI [14]. We used transmission electron microscopy to observe pyroptosis in proximal tubular cells at the ultrastructural level. Figures 2a and b show that membrane pores formed in kidney tissues in the IR group, as well as swollen mitochondria, which confirmed the occurrence of pyroptosis in the IR group. These changes were significantly alleviated by disulfiram pretreatment.

Disulfiram-mediated inhibition of pyroptosis was associated with inhibition of the caspase-11-GSDMD pathway

Studies have shown that the caspase-11-GSDMD pyroptosis pathway plays an important role in IR-induced AKI [14]. We next verified whether disulfiram mitigated kidney IR injury *via* the caspase-11-GSDMD pathway. As shown in Figure 3a–d, compared with the sham group, the protein levels of the classical pathway (ASC, NLRP3,

pro-caspase-1, caspase-1 and N-GSDMD) and nonclassical pathway (caspase-11 and N-GSDMD) were obviously elevated in the IR group. However, compared with the IR group, only all proteins in the nonclassical pathway were significantly downregulated when classical pyroptosis-associated proteins ASC and NLRP3 showed no significance in the IR + DSF group. In addition, IR notably induced IL-1 β and IL-18 expression, while disulfiram prevented this increase (Figure 3e).

Immunofluorescence staining showed an upregulation in caspase-11 and GSDMD in tubular epithelial cells in IR group, and both proteins were enriched in the same cells (Figure 3f), which indicated that nonclassical pyroptosis occurred in a certain number of kidney tubular cells after IR injury. However, the IR-induced increase in protein expression was alleviated by disulfiram treatment. Moreover, compared with the sham group, there were notable green signals indicating GSDMD protein in the tubulointerstitial area in the IR group, which were probably pyroptotic bodies, and this increase was suppressed by disulfiram treatment.

The expression of inflammatory factors in mouse renal tissue was quantified by quantitative real-time PCR. The results showed that the levels of IL-1 β and IL-18 were elevated in the IR group, while the anti-inflammatory factors IL-4 and IL-10 were downregulated. In contrast, treatment with disulfiram decreased inflammatory cytokines and increased noninflammatory factors (Figure 4).

The protective effect of disulfiram on MTECs in vitro

To measure the cytotoxicity of disulfiram pretreatment toward MTECs, we determined cell viability by using a CCK8 assay kit. The results indicated that 0.1–5 μ M disulfiram had no toxic effects on MTECs (Figure 5a). Therefore, we used 5 μ M disulfiram for subsequent experiments. The CCK8 assay results indicated that the viability in the HR group was lower than that in the control group, and this effect was ameliorated by pretreatment with disulfiram (Figure 5b).

It is well known that a large amount of ROS is produced by organ reperfusion in kidney IR models, resulting in excessive oxidative stress that exacerbates cell damage [15]. Consistently, the flow cytometry results indicated that the cellular HR model showed increased ROS levels after reoxygenation. In contrast, ROS levels in cells that were pretreated with disulfiram were significantly lower than those in the HR group (Figure 5c).

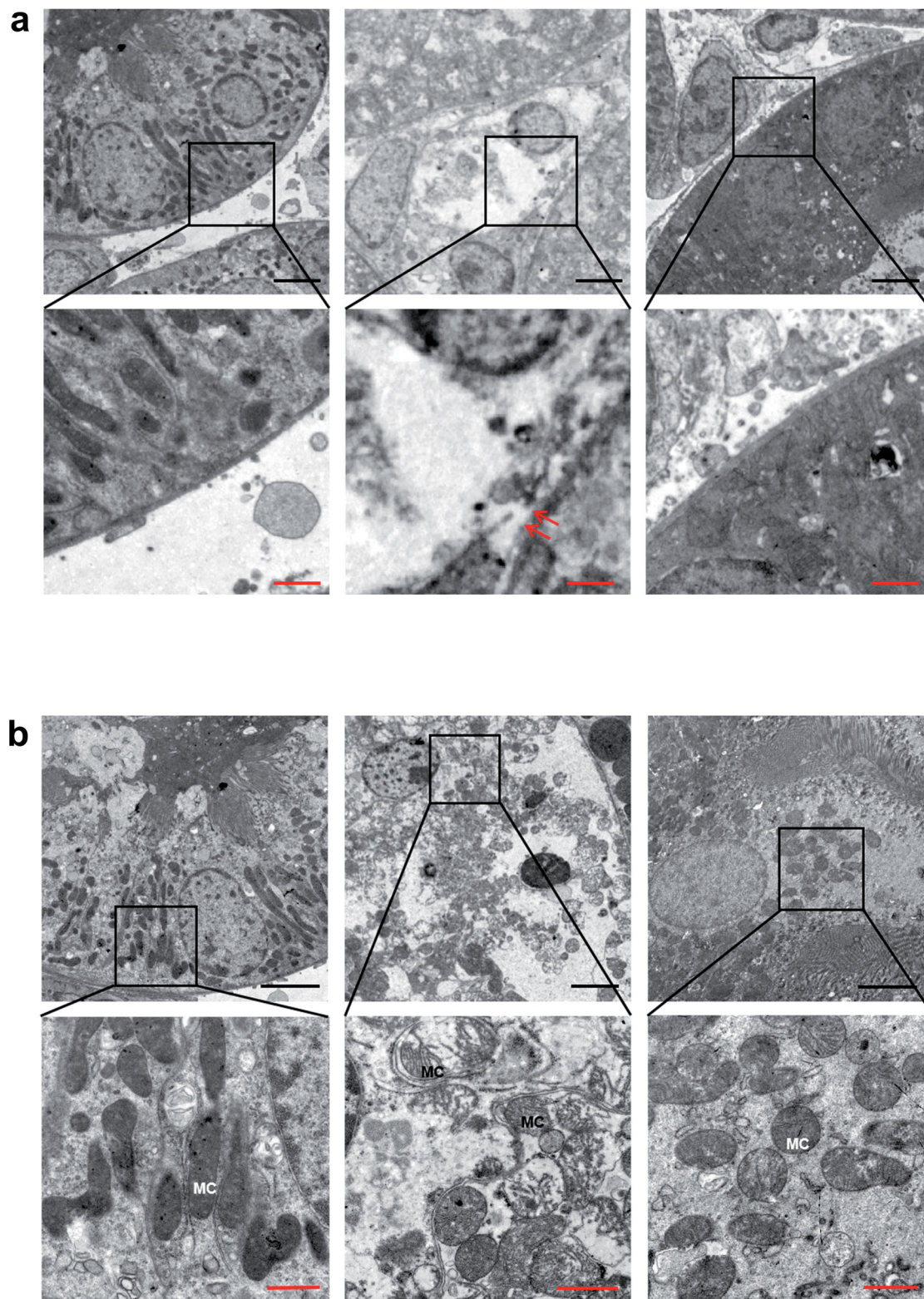


Figure 2. Representative transmission electron micrographs showing the proximal tubular cell ultrastructure of kidney sections. (a) Cytoplasmic membrane pores were observed in the proximal renal tubule after IR, and fewer were observed in the IR + DSF group. (b) Swollen mitochondria with dilated cristae were observed in the IR group, but fewer were observed in the IR + DSF group. Scale bar: black 4 μm , red 1 μm . Red double arrows: membrane pore; MC: intracellular mitochondria.

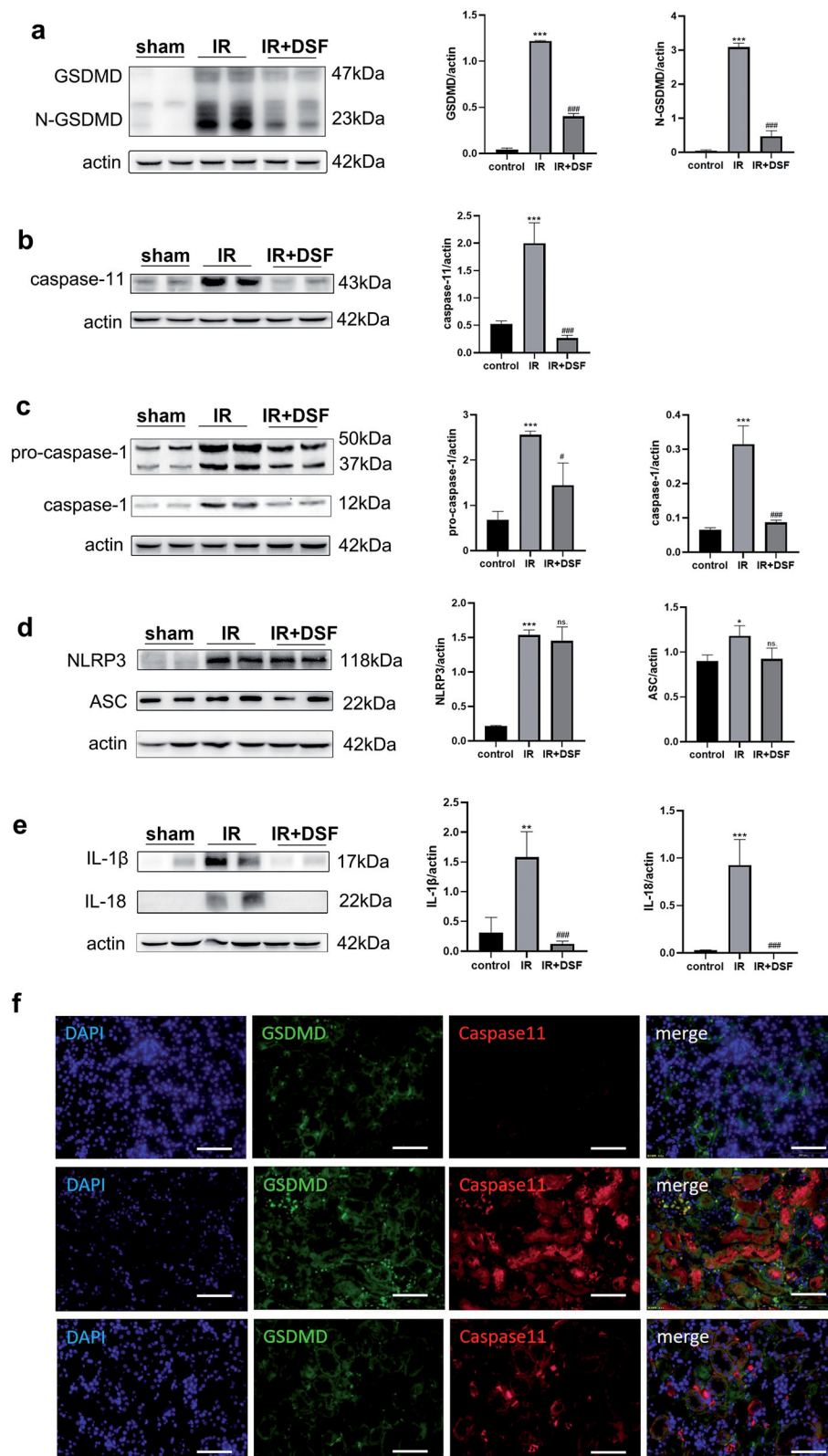


Figure 3. Disulfiram can regulate pyroptosis through the caspase-11-GSDMD pathway *in vivo*. (a) Western blot analysis of GSDMD and N-GSDMD expression. (b) Western blot analysis of caspase-11 expression. (c) Western blot analysis of caspase-1 expression. (d) Western blot analyses of NLRP3 and ASC expression. (e) Western blot analysis of IL-1 β and IL-18 expression. Protein expression was quantified by densitometric analysis. Each bar represents the mean \pm SEM of three independent experiments. (f) Immunofluorescence analysis of the expression of caspase-11 and GSDMD in kidney tissues. Scale bar = 100 μ m. * P < 0.05, ** P < 0.01, *** P < 0.001 vs. sham; # P < .05, ### P < 0.001 vs. IR. ns, no significance.

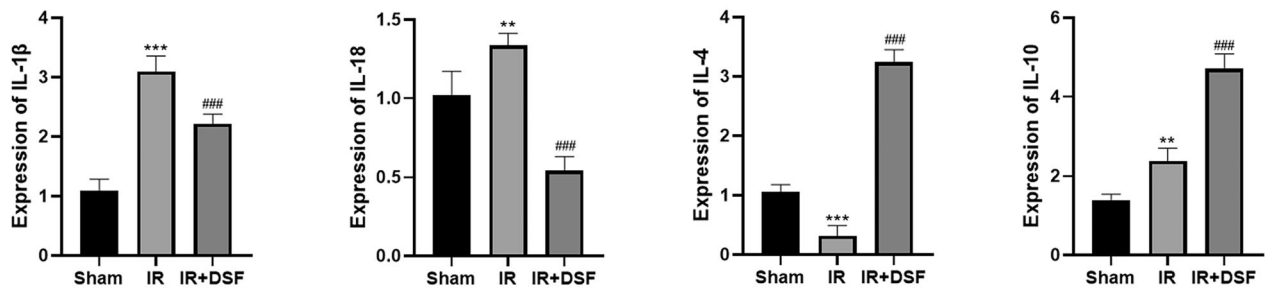


Figure 4. The regulatory effects of disulfiram on inflammatory factors were positive. (a) IL-1 β , IL-18, IL-4 and IL-10 levels were determined by RT-PCR. Each bar represents the mean \pm SEM of three independent experiments. ** $P < 0.01$, *** $P < 0.001$ vs. sham; ### $P < 0.001$ vs. IR.

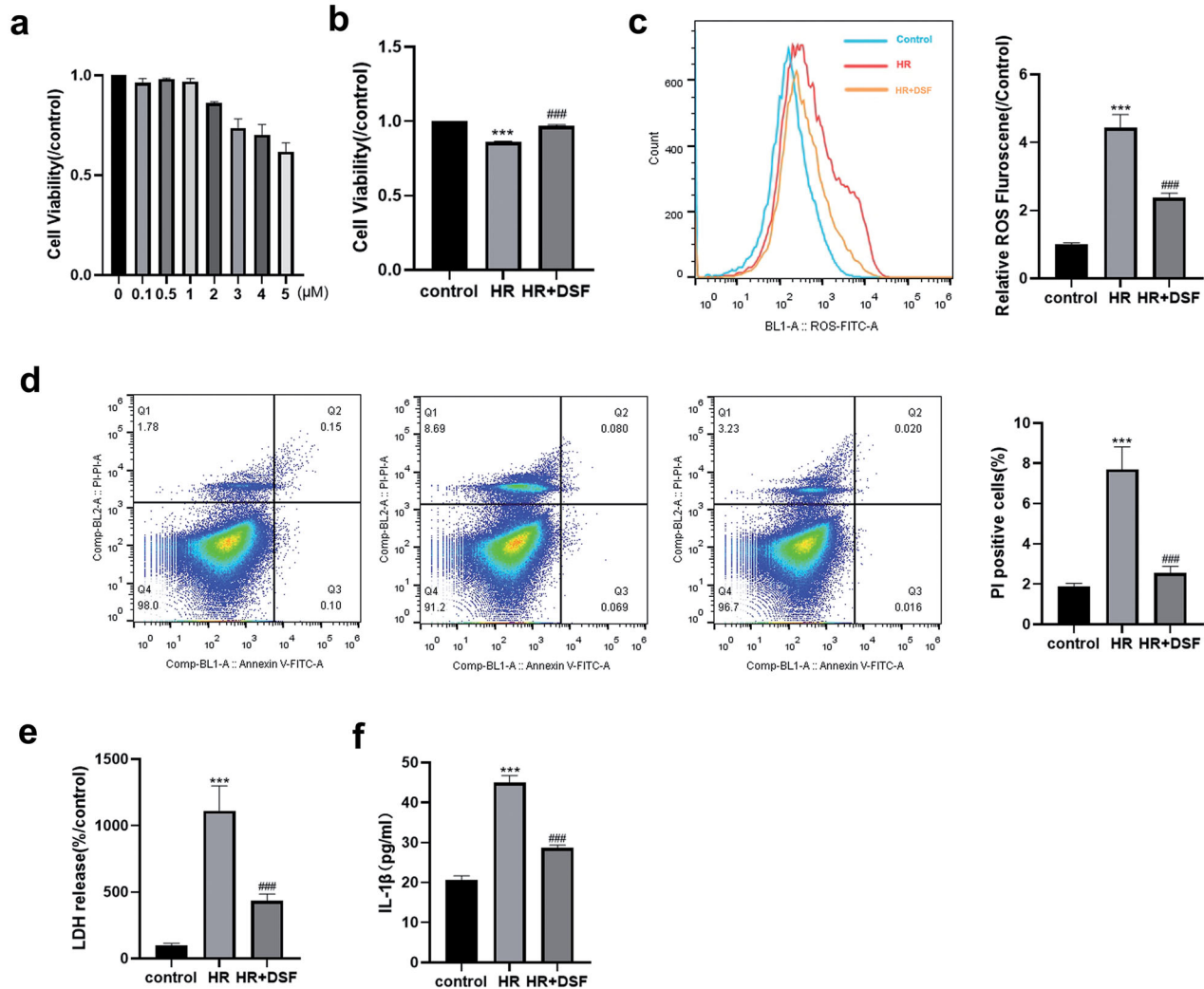


Figure 5. Disulfiram attenuated HR-induced pyroptosis in MTECs. (a, b) Cell viability was assessed by using CCK8 assays and then measured by optical density. (c) Intracellular ROS levels were quantified using DCFH-DA for 30 min after the different treatments. (d) Propidium iodide (PI) staining. (e) The percentage of LDH release was calculated as follows: $100 \times (\text{experimental LDH} - \text{spontaneous LDH}) / (\text{control LDH} - \text{spontaneous LDH})$. (f) Supernatant IL-1 β levels were measured by ELISA. Each bar represents the mean \pm SEM of three independent experiments. ** $P < 0.01$, *** $P < 0.001$ vs. control; ### $P < 0.001$ vs. HR.

Pretreatment with disulfiram suppressed HR-induced pyroptosis in MTECs

We then determined whether HR-induced cell injury activated MTEC pyroptosis. As shown in Figure 5e and f,

there were a significant increase in LDH and IL-1 β levels in the cell supernatant in the HR group. Moreover, the percentage of PI staining was correspondingly increased (Figure 5d). These observations indicated that

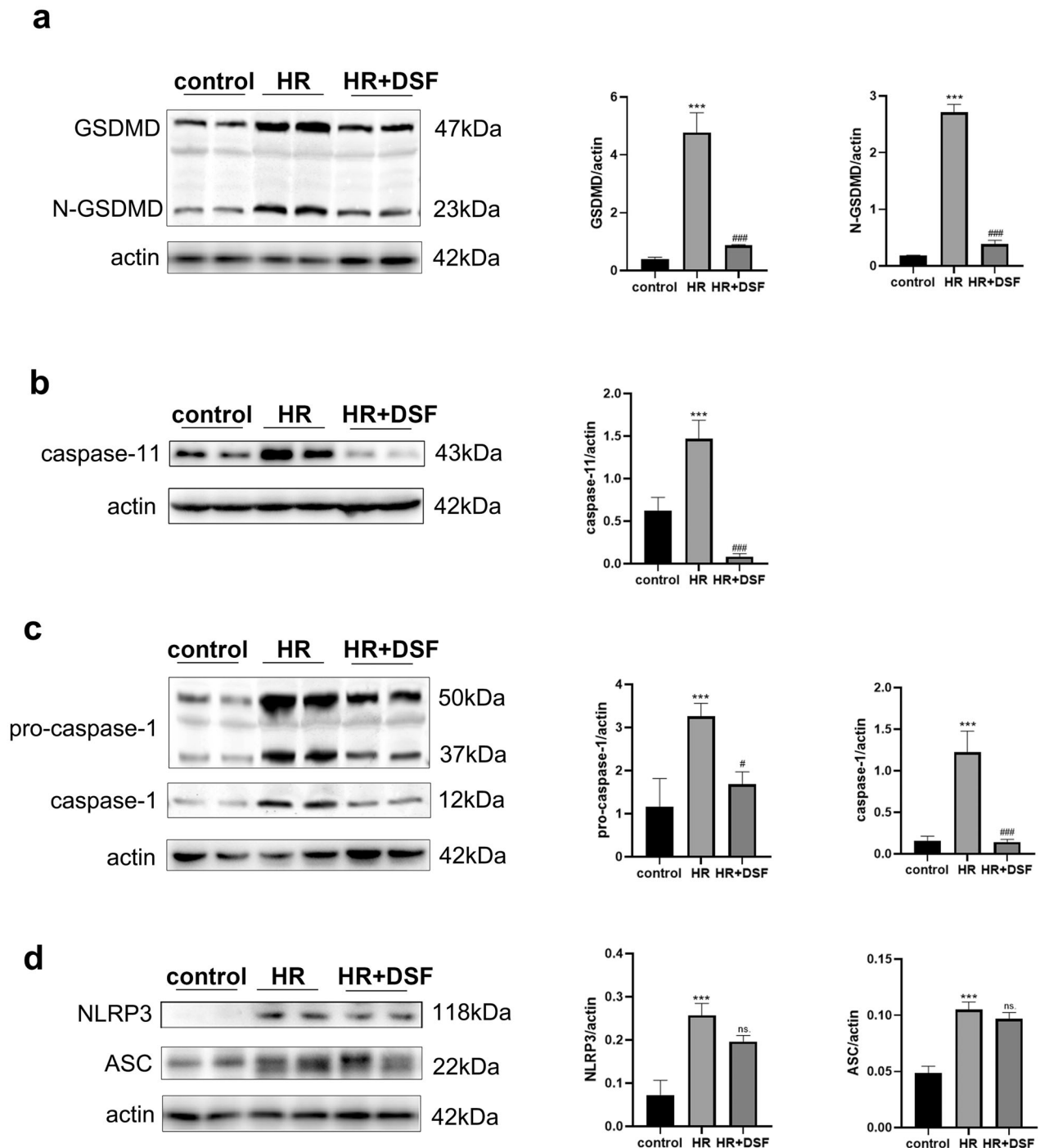


Figure 6. Disulfiram might regulate pyroptosis through the caspase-11-GSDMD pathway *in vitro*. (a) Western blot analysis of N-GSDMD expression. (b) Western blot analyses of caspase-11 expression. (c) Western blot analysis of caspase-1 expression. (d) Western blot analysis of NLRP3 and ASC expression. Protein expression was quantified by densitometric analysis. Each bar represents the mean \pm SEM of three independent experiments. *** $P < 0.001$ vs. control; # $P < 0.05$, ### $P < 0.001$ vs. HR. ns, no significance.

pyroptosis was activated in HR-induced MTEC injury, and these effects could be partially reversed by pre-treatment with disulfiram.

Disulfiram relieved HR-induced pyroptosis through the caspase-11-GSDMD pathway

As shown in Figures 5 and 6, compared to those in the control group, the protein levels of caspase-1, caspase-

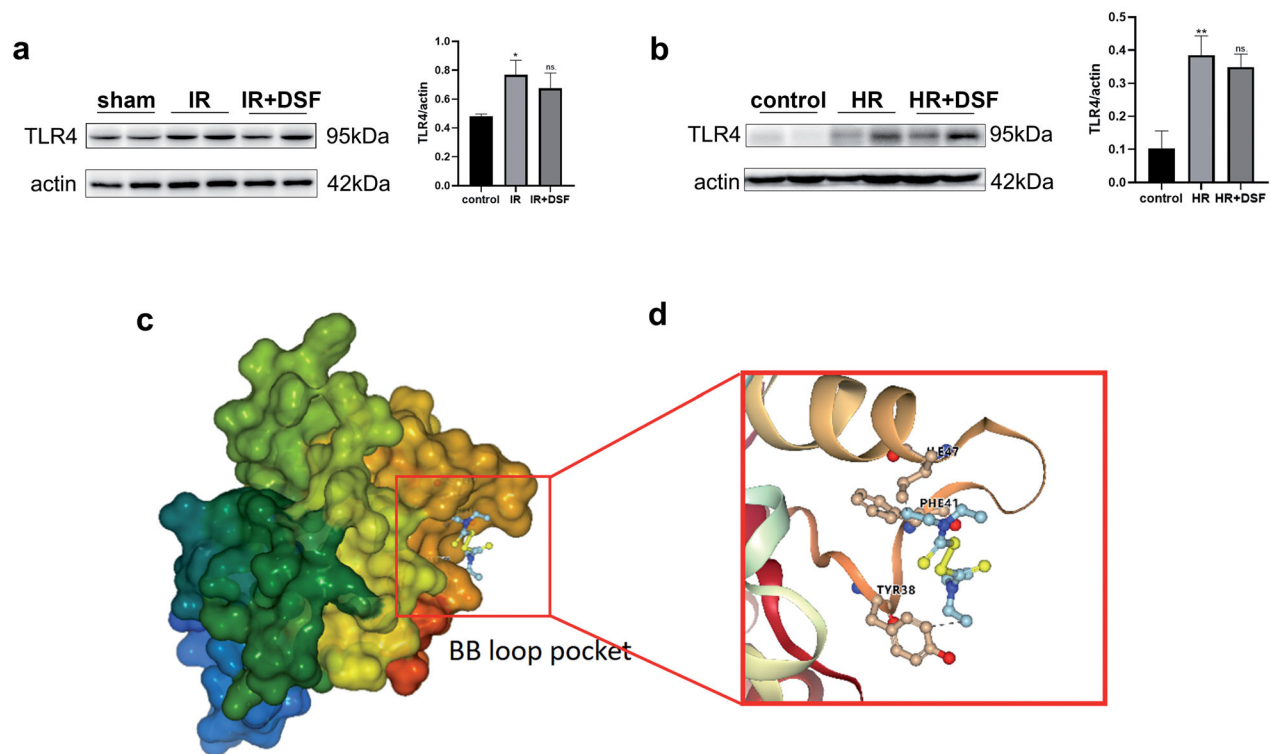


Figure 7. Molecular docking showed the potential binding of disulfiram to the TIR domain. (a) Western blot analysis of TLR4 expression *in vivo*. (b) Western blot analysis of TLR4 expression *in vitro*. (c) Homology modeling of the 3D structure of the TIR domain. (d) A docking pose of disulfiram in the binding pocket close to the BB loop. Protein expression was quantified by densitometric analysis. Each bar represents the mean \pm SEM of three independent experiments. ** $P < 0.01$, *** $P < 0.001$ vs. control. ns, no significance.

11 and GSDMD and the cell supernatant concentrations of IL-1 β were increased in the HR group. When the cells were pretreated with disulfiram, the expression levels of caspase-11 and GSDMD were significantly decreased (Figure 6a and b), while NLRP3 and ASC expression levels were not significantly changed (Figure 6d). Therefore, these results suggest that the protective effect of disulfiram against kidney IR injury might be related to the caspase-11-GSDMD pathway.

Discussion

In our study, kidney IR injury increased Scr and BUN levels and tubular structure damage. Evidence of proximal tubular cell pyroptosis was observed in the IR group using transmission electron microscopy. Pyroptotic proteins such as TLR4, NLRP3, ASC, caspase-1, caspase-11, and N-GSDMD were also increased after IR injury. Disulfiram pretreatment alleviated kidney IR injury, decreased the protein expression of the caspase-11-GSDMD axis and caspase-1, and reduced the leakage of IL-1 β and IL-18. However, some classical pyroptosis proteins, such as NLRP3 and ASC, showed no significant

differences after treatment with disulfiram. Our results suggested that the protective effect of disulfiram on kidney IR injury was related to the inhibition of the caspase-11-GSDMD pathway.

IR-AKI often occurs after major surgery, which often requires the use of anti-infective drugs and various anti-coagulants. After consulting the literature, we found that disulfiram is easy to react with other drugs, leading to adverse effects. Disulfiram may affect the time of action of prothrombin [16], and psychotic reactions need to be closely watched when disulfiram is used in combination with antibacterial drugs such as metronidazole [17] or isoniazid [18]. Therefore, the use of disulfiram is best to avoid other drugs. That's why we used the pretreatment of disulfiram in this experiment.

Kidney IR injury-induced cell death involves multiple forms of cell death, including pyroptosis [4,19]. The concept of pyroptosis is now being considered a kind of gasdermin-protein-dependent regulated cell death [20,21], which is often but not always accomplished by the activation of inflammatory caspases [22]. Kidney tubular cell pyroptosis is not confined to the renal area. Severe damage can also release damage-related

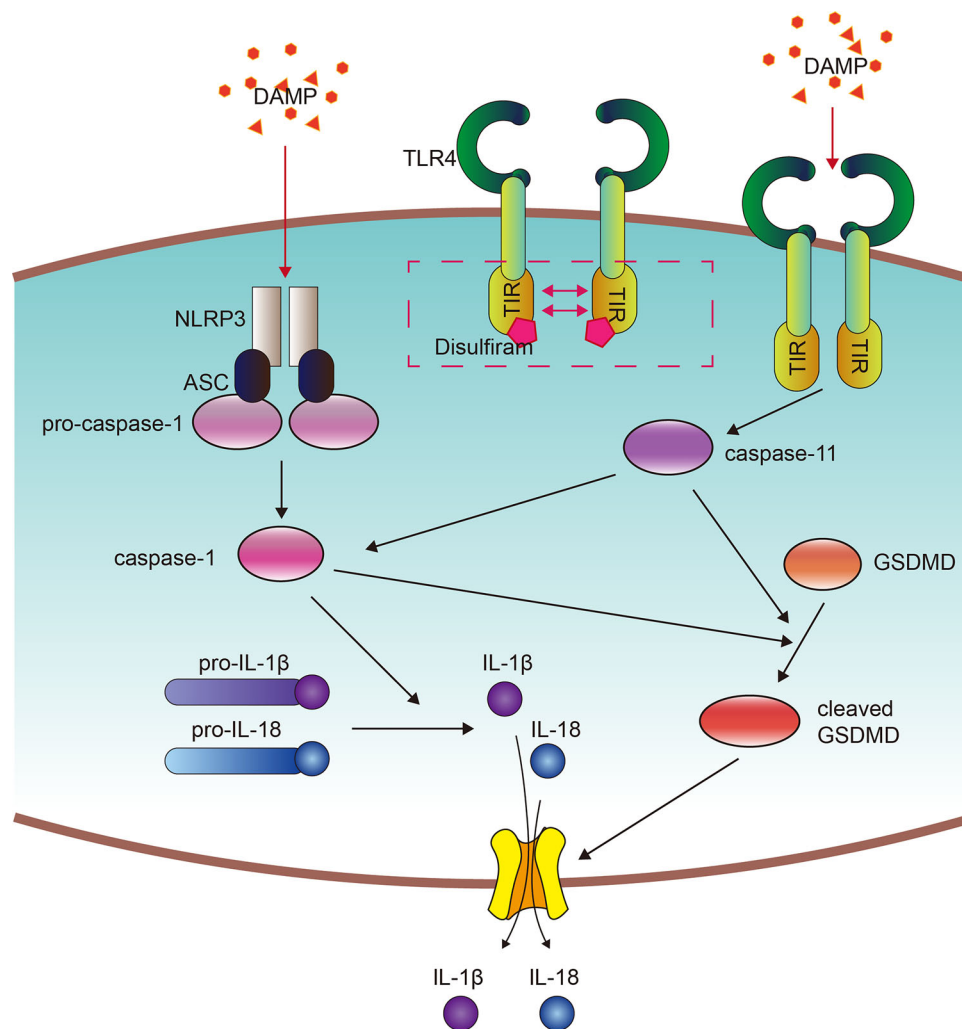


Figure 8. Concept map showing kidney IR-induced pyroptosis signaling and the protective effect of disulfiram. Kidney I/R injury or H/R induced pyroptotic cell death signaling, including the upregulation of the classical pathway and nonclassical pathway. Disulfiram treatment ameliorated IR-induced AKI by regulating the caspase-11-GSDMD pathway. The arrows represent promotion.

molecular patterns (DAMPs) and cellular fragments into the circulation and cause distant organ impairment, such as acute liver injury [23].

GSDMD is one of the effector proteins of pyroptosis. To date, two mechanisms explain the interpretation of GSDMD membrane pore formation and the inflammatory response [24,25]. One is the classical pathway, which is the typical NLRP3 inflammasome pathway. The NLRP3 inflammasome can recognize diverse DAMPs and pathogen-associated molecular patterns (PAMPs) and bind to pro-caspase-1 through ASC; then, caspase-1 is generated by the cleavage of pro-caspase-1, which results in the maturation of IL-1 β and IL-18 [26,27]. The other pathway is the nonclassical inflammasome pathway, in which PAMPs (such as LPS) activate caspase-11 (human caspase-4 and caspase-5) directly or through TLR4 [24]. In our study, we confirmed the activation of these two inflammasome pathways in a kidney IR injury model. However, there were some specific

circumstances in our experiment. After disulfiram treatment, we confirmed that caspase-1, GSDMD and mature IL-1 β and IL-18 were significantly decreased, but the expression of ASC and NLRP3 did not change significantly after drug administration. We hypothesized that the downregulation of caspase-1 expression was incidental to the reduction in caspase-11 since caspase-11 was also involved in the regulation of caspase-1 formation [28–30].

IR injury often occurs in sterile environments, but the process has many similarities to the activation of the host immune response to microbial invasion [31,32]. For example, the receptor TLR4 could also be activated by endogenous molecules from nonmicrobial compounds during IR, and these ligands are called DAMPs [33]. When tissue is damaged, DAMPs are released into the intercellular space to activate the downstream TLR4-related immune response. Some studies have shown that TLR4 is required for the upregulation of

caspase-11 expression [34]; therefore, the decrease in caspase-11 after disulfiram administration in our study might be associated with the antagonism of TLR4.

TLR4 was reported to be activated by DAMPs in kidney IR injury [35]. We measured TLR4 expression in the IR and HR models by western blotting (Figure 7a and b) and found that TLR4 protein expression was significantly upregulated in both models, while treatment with disulfiram did not reduce TLR4 expression. The TLR4 protein structure is divided into three domains: extracellular receptors, transmembrane domains, and intracellular receptors. In the presence of DAMPs, the intracellular segment of the TLR4-TIR domain dimerizes, enabling TLR4 activation and upregulating caspase-11 expression. The flexible BB loop of the TIR domain (the region between the α B chain and β B chain) may be the site of TIR dimerization, and mutations in this region could seriously affect the function of proteins containing TIR domains [36]. Therefore, it is reasonable to hypothesize that disulfiram may inhibit TLR4 activation by affecting the dimerization of the TIR domain, thus reducing the upregulation of caspase-11 expression. We established a protein model of the TIR domain by the homology modeling method. Through flexible molecular docking, we found that disulfiram could bind to the BB loop pocket of the TIR protein through hydrophobic interactions (Figure 7c and d), which may affect the conformation of the loop, thus affecting the binding of downstream proteins.

Recently, there have been some new inhibitors against caspase, such as Z-VAD-FMK [37], VX-765 [38] and wedelolactone [39], but they are all expensive. Functional exploration of old drugs means reduced costs for the research and development of new pharmaceuticals. New functions of the old medicine disulfiram are still being discovered. In the present study, we found that disulfiram has an inhibitory effect on the caspase-11-GSDMD pathway in kidney IR injury, indicating that it is a promising antiapoptotic drug.

In summary, we revealed that disulfiram ameliorated renal IR injury by inhibiting the caspase-11-GSDMD axis and cell pyroptosis (Figure 8), which suggested that it could be a promising therapeutic agent against AKI. However, the specific molecular mechanism by which disulfiram downregulates caspase-11 expression is still unclear, and the computer simulation showing disulfiram and TLR4 binding still need further experimental confirmation.

Disclosure statement

The authors declare that there are no conflicts of interest.

Funding

This work was funded by the National Natural Science Foundation of China (81970667, 81900610) and Outstanding Key Member Program of Zhongshan Hospital, Fudan University (2021ZSGG09).

References

- [1] Ronco C, Bellomo R, Kellum JA. Acute kidney injury. *Lancet*. 2019;394(10212):1949–1964.
- [2] Rewa O, Bagshaw SM. Acute kidney injury-epidemiology, outcomes and economics. *Nat Rev Nephrol*. 2014;10(4):193–207.
- [3] Hoste E, Kellum JA, Selby NM, et al. Global epidemiology and outcomes of acute kidney injury. *Nat Rev Nephrol*. 2018;14(10):607–625.
- [4] Han SJ, Lee HT. Mechanisms and therapeutic targets of ischemic acute kidney injury. *Kidney Res Clin Pract*. 2019;38(4):427–440.
- [5] Tajima T, Yoshifuji A, Matsui A, et al. β -hydroxybutyrate attenuates renal ischemia-reperfusion injury through its anti-pyrototic effects. *Kidney Int*. 2019;95(5):1120–1137.
- [6] Petersen EN. The pharmacology and toxicology of disulfiram and its metabolites. *Acta Psychiatr Scand Suppl*. 1992;369:7–13.
- [7] Paik S, Kim JK, Silwal P, et al. An update on the regulatory mechanisms of NLRP3 inflammasome activation. *Cell Mol Immunol*. 2021;18(5):1141–1160.
- [8] Cockram PE, Kist M, Prakash S, et al. Ubiquitination in the regulation of inflammatory cell death and cancer. *Cell Death Differ*. 2021;28(2):591–605.
- [9] Kranzler HR, Soyka M. Diagnosis and pharmacotherapy of alcohol use disorder: a review. *JAMA*. 2018;320(8):815–824.
- [10] Kannappan V, Ali M, Small B, et al. Recent advances in repurposing disulfiram and disulfiram derivatives as copper-dependent anticancer agents. *Front Mol Biosci*. 2021;8:741316.
- [11] Hu JJ, Liu X, Xia S, et al. FDA-approved disulfiram inhibits pyroptosis by blocking gasdermin D pore formation. *Nat Immunol*. 2020;21(7):736–745.
- [12] Lang PT, Brozell SR, Mukherjee S, et al. DOCK 6: combining techniques to model RNA-small molecule complexes. *RNA*. 2009;15(6):1219–1230.
- [13] Mukherjee S, Balius TE, Rizzo RC. Docking validation resources: protein family and ligand flexibility experiments. *J Chem Inf Model*. 2010;50(11):1986–2000.
- [14] Miao N, Yin F, Xie H, et al. The cleavage of gasdermin D by caspase-11 promotes tubular epithelial cell pyroptosis and urinary IL-18 excretion in acute kidney injury. *Kidney Int*. 2019;96(5):1105–1120.
- [15] Chen W, Li D. Reactive oxygen species (ROS)-responsive nanomedicine for solving ischemia-reperfusion injury. *Front Chem*. 2020;8:732.
- [16] O'Reilly RA. Interaction of sodium warfarin and disulfiram (antabuse) in man. *Ann Intern Med*. 1973;78(1):73–76.

- [17] Goodhue WW. Jr. Disulfiram-metronidazole (well identified) toxicity. *N Engl J Med.* 1969;280(26):1482–1483.
- [18] Whittington HG, Grey L. Possible interaction between disulfiram and isoniazid. *Am J Psychiatry.* 1969; 125(12):1725–1729.
- [19] Jun W, Benjanuwattra J, Chattipakorn SC, et al. Necroptosis in renal ischemia/reperfusion injury: a major mode of cell death. *Arch Biochem Biophys.* 2020;689:108433.
- [20] Christgen S, Tweedell RE, Kanneganti TD. Programming inflammatory cell death for therapy. *Pharmacol Ther.* 2022;232:108010.
- [21] Shi J, Gao W, Shao F. Pyroptosis: gasdermin-mediated programmed necrotic cell death. *Trends Biochem Sci.* 2017;42(4):245–254.
- [22] Shi J, Zhao Y, Wang K, et al. Cleavage of GSDMD by inflammatory caspases determines pyroptotic cell death. *Nature.* 2015;526(7575):660–665.
- [23] Tonnus W, Gemhardt F, Latk M, et al. The clinical relevance of necroinflammation-highlighting the importance of acute kidney injury and the adrenal glands. *Cell Death Differ.* 2019;26(1):68–82.
- [24] Rathinam V, Zhao Y, Shao F. Innate immunity to intracellular LPS. *Nat Immunol.* 2019;20(5):527–533.
- [25] Chauhan D, Vande Walle L, Lamkanfi M. Therapeutic modulation of inflammasome pathways. *Immunol Rev.* 2020;297(1):123–138.
- [26] Jo EK, Kim JK, Shin DM, et al. Molecular mechanisms regulating NLRP3 inflammasome activation. *Cell Mol Immunol.* 2016;13(2):148–159.
- [27] Haneklaus M, O'Neill LA. NLRP3 at the interface of metabolism and inflammation. *Immunol Rev.* 2015; 265(1):53–62.
- [28] Miao NJ, Xie HY, Xu D, et al. Caspase-11 promotes renal fibrosis by stimulating IL-1 β maturation via activating caspase-1. *Acta Pharmacol Sin.* 2019;40(6): 790–800.
- [29] Wang S, Miura M, Jung YK, et al. Murine caspase-11, an ICE-interacting protease, is essential for the activation of ICE. *Cell.* 1998;92(4):501–509.
- [30] Kang SJ, Wang S, Hara H, et al. Dual role of caspase-11 in mediating activation of caspase-1 and caspase-3 under pathological conditions. *J Cell Biol.* 2000;149(3): 613–622.
- [31] Fernández AR, Sánchez-Tarjuelo R, Cravedi P, et al. Review: ischemia reperfusion injury-A translational perspective in organ transplantation. *Int J Mol Sci.* 2020;21(22):8549.
- [32] Weigt SS, Palchevskiy V, Belperio JA. Inflammasomes and IL-1 biology in the pathogenesis of allograft dysfunction. *J Clin Invest.* 2017;127(6):2022–2029.
- [33] Sepe V, Libetta C, Gregorini M, et al. The innate immune system in human kidney inflammaging. *J Nephrol.* 2022;35(2):315–381.
- [34] Broz P, Ruby T, Belhocine K, et al. Caspase-11 increases susceptibility to salmonella infection in the absence of caspase-1. *Nature.* 2012;490(7419):288–291.
- [35] Zheng M, Ambesi A, McKeown-Longo PJ. Role of TLR4 receptor complex in the regulation of the innate immune response by fibronectin. *Cells.* 2020;9(1):216.
- [36] Saqib U, Baig MS. Identifying the inhibition of TIR proteins involved in TLR signalling as an anti-inflammatory strategy. *SAR QSAR Environ Res.* 2018;29(4): 295–318.
- [37] Chang H, Sun F, Tian K, et al. Caspase inhibitor z-VAD-FMK increases the survival of hair cells after Actinomycin-D-induced damage in vitro. *Neurosci Lett.* 2020;732:135089.
- [38] McKenzie BA, Mamik MK, Saito LB, et al. Caspase-1 inhibition prevents glial inflammasome activation and pyroptosis in models of multiple sclerosis. *Proc Natl Acad Sci USA.* 2018;115(26):E6065–E6074.
- [39] Kobori M, Yang Z, Gong D, et al. Wedelolactone suppresses LPS-induced caspase-11 expression by directly inhibiting the IKK complex. *Cell Death Differ.* 2004; 11(1):123–130.